Physica Scripta. Vol. 41, 38–41, 1990.

Spin-Resolved Photoionisation of Lead Above the $Pb^+ (6s^2 6p)\ ^2P_{3/2}$-Threshold

M. Müller, N. Böwering, F. Schäfers* and U. Heinzmann

Fakultät für Physik der Universität Bielefeld, D-4800 Bielefeld, Federal Republic of Germany: Fritz-Haber-Institut der MPG, D-1000 Berlin 33, Federal Republic of Germany; *BESSY, Lentzeallee 100, D-1000 Berlin 33, Federal Republic of Germany

Received July 16, 1989; accepted September 14, 1989

Abstract

The spin-polarisation parameters for photoelectrons from lead atoms $(6s^2 6p^2)_{J=0}$ were measured in the wavelength range between the second threshold $[Pb^+ (6s^2 6p)\ ^2P_{3/2}]$ and 100 nm in an angle-resolving experiment using circularly polarised vuv-radiation from the storage ring BESSY. Beyond this threshold (λ = 135.3 nm), the photoionisation cross section is strongly perturbed by autoionisation resonances. Especially, a strong enhancement of the generally weak $Pb^+ (6s^2 6p)\ ^2P_{3/2}$ photoionisation cross section occurs. Theoretical calculations by Radojevic [15] attribute these resonances to the $6s6p^3$-configuration of lead. By use of the measured spin-polarisation parameters A, ξ and α which show pronounced variations in the region investigated for both final ionic states $^2P_{1/2}$ and $^2P_{3/2}$ a detailed discussion of the resonances is performed.

1. Introduction

In the last decade the investigation of the photoionisation process with detection of the spin polarisation of the outgoing photoelectrons has become a suitable method for analysing electronic structure [1]. In general, the experimental determination of the spin-polarisation vector yields the three independent spin-parameters A, ξ and α, which allow a deeper insight in the photoionisation dynamics [1]. Especially in the atomic case, these data (A, ξ and α) in connection with the total cross section σ and the intensity-asymmetry parameter β form a set for a complete quantum-mechanical characterisation of the photoionisation process [2–6].

In this paper we present experimental results for the spin-polarisation parameters A, ξ and α and the intensity-asymmetry parameter β of lead in the wavelength region from the second ionisation threshold $^2P_{3/2}$ (135.3 nm) [10] up to λ = 100 nm. The ground state of $Pb(6s^2 6p^2)_{J=0}$ represents a typical case of a multiconfiguration state. Following *jj*-coupling the ground state is given by [7–9]:

$$\Psi = [c_1 \Psi(6p_{1/2}^2) + c_2 \Psi(6p_{3/2}^2)]_{J=0}. \quad (1)$$

where c_1 and c_2 denote the mixing coefficients (with $c_1^2 + c_2^2 = 1$). Thus, the photoionisation of the $6p^2$-shell results in two final ionic states $Pb^+ (6s^2 6p)\ ^2P_{1/2}$ and $^2P_{3/2}$ with thresholds of 167.2 nm (7.42 eV) and 135.3 nm (9.16 eV), respectively [10].

The mixing amplitude c_2^2 for the $(6p_{3/2})^2$ configuration in the ground state is about 7%, as shown by experiment [7, 9]. Therefore, the dominating channel in photoionisation of the p^2-shell is the final ionic state $Pb^+ (6s^2 6p)\ ^2P_{1/2}$. Recent observation of Krause *et al.* [11] shows, however, that in the region above the second threshold strong autoionisation resonances occur, which "enhance" the photoionisation cross section of the other channel with $^2P_{3/2}$. These resonances were not observed in absorption measurements [10, 12–14]. In the work of Krause *et al.* [11] the origin of these resonances is attributed to the $6s6p^3$-configuration of lead. A Multiconfiguration Dirac–Fock (MCDF) calculation of Radojevic [15] for the energetic position of the $6s6p^3$-configuration states supports the assumption of Krause *et al.* [11]. The assignments given by Radojevic take into account that the lead atoms are partly in an excited state: $\hat{c}^2\ \Psi(6s^2 6p^2)_{J=0}$, $\Delta E = 36\,000\ \mathrm{cm}^{-1}$ (same configuration as in the ground state [see equation (1)], but different occupation: $\hat{c}^2 \sim 93\%$). The population of the excited states in an experiment is explained by collisions (ion-atom) in the target region since the thermal population is negligible at typical evaporation temperatures of 1000–1100 K [9, 11].

Up to now only photoelectron intensity measurements were performed in this resonance region [11] and a detailed discussion was not possible. By use of the measured values for the spin-polarisation parameters A, ξ and α a detailed insight in the decay mechanism with respect to the two final ionic states can be obtained.

2. Experimental

The experiment was carried out at the electron storage ring BESSY with circularly polarised VUV off plane synchrotron radiation using the 6.5 m normal incidence monochromator ($\Delta\lambda$ = 0.5 nm) [16]. The monochromatic light hits the atomic beam of lead (purity = 99.96%, evaporation temperature $T_{Pb} \sim 1100$ K) and the photoelectrons produced are analysed with respect to their kinetic energy distribution corresponding to the emission angle Θ by a rotatable electron spectrometer [17]. (The reaction plane is spanned by the momenta of incoming photon and analysed photoelectron.) After two electrostatic deflections the electron beam is focused into a spatially fixed electron lens system, accelerated to 100 keV and scattered on the gold foil of the Mott detector. From the measured intensity asymmetries in the 4 backward counters the two transverse spin-polarisation components $A(\Theta)$ and $P_\perp(\Theta)$ are simultaneously determined. Details of the rotatable electron spectrometer system and the Mott detector for spin-polarisation analysis are given elsewhere [6, 17]. The analytical dependences of $A(\Theta)$ (component in the direction of the incident photon beam) and $P_\perp(\Theta)$ (component perpendicular to the reaction plane) in our geometry are given by the following equations [18, 19]:

$$A(\Theta) = \gamma \frac{A - \alpha P_2[\cos(\Theta)]}{1 - \beta/2 P_2[\cos(\Theta)]} \quad (2a)$$

$$P_\perp(\Theta) = \frac{2\xi \cos(\Theta) \sin(\Theta)}{1 - \beta/2 P_2[\cos(\Theta)]} \quad (2b)$$

with $\gamma = \pm 1$ = helicity of light, $P_2[\cos(\Theta)]$ = second Legendre polynominal, β = angular asymmetry parameter of photoelectron intensity, A, ξ, α = photoelectron spin-polarisation parameters.

By measuring at the magic-angle, $\Theta_m = 54°44'$, where $P_2[\cos(\Theta)] = 0$, one obtains directly the spin-polarisation parameters A and ξ, whereas the third spin-polarisation parameter α and the intensity-asymmetry parameter β are determined by fitting the angular dependence of $A(\Theta)$ [cf. equation (2a)]. However the fitting procedure is less sensitive with respect to the β parameter than direct angular resolved photoemission intensity measurements (proportional to the denominator in equation (2a)).

3. Results and discussion

The investigated photoionisation process of lead atoms $Pb(6s^2 6p^2)$ is described by the following reaction scheme:

<u>*ground state:*</u>

$Pb(6s^2 6p^2)_{J=0} + h\nu(\sigma^+, \sigma^-)$

<u>*autoionisation states:*</u>

$\longrightarrow [Pb^*(6s6p^3)]_{J=1}$ (3a)

<u>*continuum states:*</u>

$\xrightarrow{h\nu \geq 7.42\,eV} [Pb^+(6s^2 6p)\ ^2P_{1/2} + \varepsilon s_{1/2}, \varepsilon d_{3/2}]_{J=1}$ (3b)

$\xrightarrow{h\nu \geq 9.16\,eV} [Pb^+(6s^2 6p)\ ^2P_{3/2} + \varepsilon s_{1/2}, \varepsilon d_{3/2}, \varepsilon d_{5/2}]_{J=1}$ (3c)

For $\lambda < 135.3$ nm the corresponding photoelectrons differ by $\Delta E = 1.74$ eV in kinetic energy due to the fine structure splitting and are readily resolved by means of the electron spectrometer.

Figure 1(a, b) show the photoelectron intensity measured for $Pb^+(6s^2 6p)\ ^2P_{1/2}$ and $Pb^+(6s^2 6p)\ ^2P_{3/2}$ between the second ionisation threshold (dotted line) and $\lambda = 100$ nm. The intensities were recorded at the magic angle $\Theta_m = 54°44'$ and are normalised with respect to the actual electron current in the storage ring and to the spectral transmission of the 6.5 m-monochromator (1200 l/mm-grating) [16].

The comparison of the intensities demonstrates clearly that the decay mechanism of these resonances differs strongly in the final ionic states. Especially, the resonance at $\lambda \sim 116.5$ m interacts mostly with the $Pb^+\ ^2P_{3/2}$ ionic channel. Within the resonance at $\lambda \sim 108$ nm a drop in intensity for the $^2P_{1/2}$-ionic channel occurs causing the shape of the resonance to be strongly asymmetric, while in the $Pb^+\ ^2P_{3/2}$-ionic channel a broad Lorentzian peak occurs.

The high value of the photoelectron intensity of the $^2P_{1/2}$ ionic channel at the $^2P_{3/2}$ threshold is attributed to the influence of autoionising Rydberg series [12] converging to this threshold and leading to a high photoionisation cross section. The pronounced decrease of the intensity ($^2P_{1/2}$-channel) above threshold is stronger than usually observed (see for example $Ar(3p^6)$ [20]). A possible reason could be a Cooper-minimum [21] in the $Pb^+\ ^2P_{1/2}$-channel.

Following the work of Radojevic [15] which locates a state of the $6s6p^3$-configuration in the vicinity of the $^2P_{3/2}$-threshold the high intensities at threshold and the decrease at shorter wavelengths for the $^2P_{1/2}$-ionic channel and the increase in intensity for the $^2P_{3/2}$-ionic channel [see Fig. 1 (a, b)] could be explained by a strong interchannel interaction

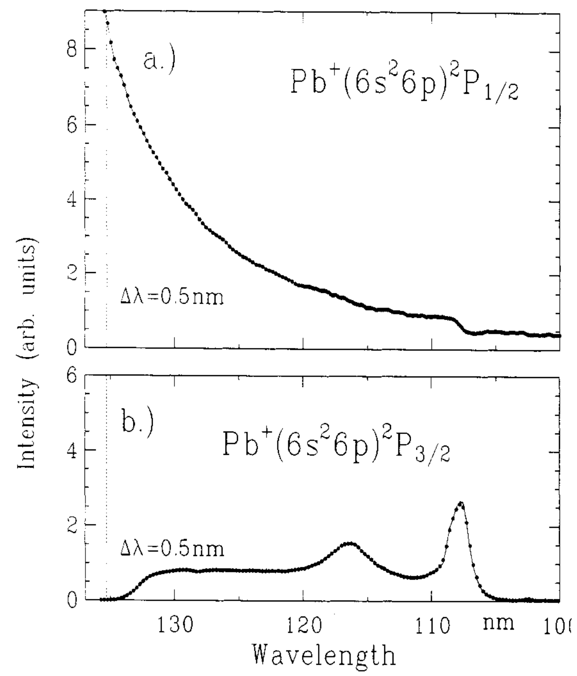

Fig. 1. (a, b) Photoelectron intensity for $Pb^+(6s^2 6p)\ ^2P_{1/2}$ and $^2P_{3/2}$ between $\lambda = 100$ nm and the second ionisation threshold (dotted line) ($\Delta\lambda = 0.5$ nm). The intensities were recorded at the magic angle ($\Theta_m = 54°44'$) and were normalized to the current of the storage ring and to the photon flux of the 6.5 m-monochromator [16]. The solid lines represent a connection of the data points to guide the eyes.

[22]. In general the measured intensities of Krause *et al.* [11] are in agreement with our data, despite the fact that the resonance at $\lambda \sim 116.5$ nm is more pronounced in the $^2P_{3/2}$-ionic channel in our work. In Fig. 2(a, b) and Fig. 3(a, b) the experimental results of the spin-polarisation parameters A, ξ, α and of the intensity-asymmetry parameter β for $Pb^+(6s^2 6p)\ ^2P_{1/2}$ and $^2P_{3/2}$, respectively, are shown in the region between the threshold and $\lambda = 100$ nm [in Fig. 3(a) in comparison with the intensity].

In the following discussion the spin-polarisation parameters and the intensity-asymmetry parameter β are labelled by $A_{1/2}$, $\xi_{1/2}$, $\alpha_{1/2}$ and $\beta_{1/2}$ for $Pb^+\ ^2P_{1/2}$ and $A_{3/2}$, $\xi_{3/2}$, $\alpha_{3/2}$ and $\beta_{3/2}$ for $Pb^+\ ^2P_{3/2}$. In the following we first discuss the results for the $Pb^+\ ^2P_{1/2}$-ionic channel. The data for the spin-polarisation parameter $A_{1/2}$ indicate an increase from negative values at the second threshold up to $A_{1/2} \sim 0$ at $\lambda = 109$ nm which is followed by a strong decrease in the resonance at $\lambda = 108$ nm. A similar decrease at $\lambda \sim 108$ nm is observed for the spin-polarisation parameters $\xi_{1/2}$ and $\alpha_{1/2}$ and the intensity-asymmetry parameter $\beta_{1/2}$. The $\xi_{1/2}$-parameter changes sign at this position; with increasing photon energy another change of sign is observed.

In the region from the second ionisation threshold to $\lambda \sim 108$ nm the $\alpha_{1/2}$- and the $\beta_{1/2}$-parameter are increasing in similar behaviour as the $A_{1/2}$-parameter. In contrast to the $A_{1/2}$-, $\alpha_{1/2}$- and $\beta_{1/2}$-parameters the $\xi_{1/2}$-parameter varies strongly; especially from $\lambda = 120$–115 nm a decrease to zero occurs which is followed by an increase with a weak variation at $\lambda \sim 110$ nm. Furthermore, in the vicinity of the threshold at $\lambda \sim 133$ nm a change of sign is observed.

It is worthwhile to note that the pronounced variation of the $\xi_{1/2}$-parameter from $\lambda = 120$–115 nm occurs in the range where a broad autoionisation resonance in the other $^2P_{3/2}$-

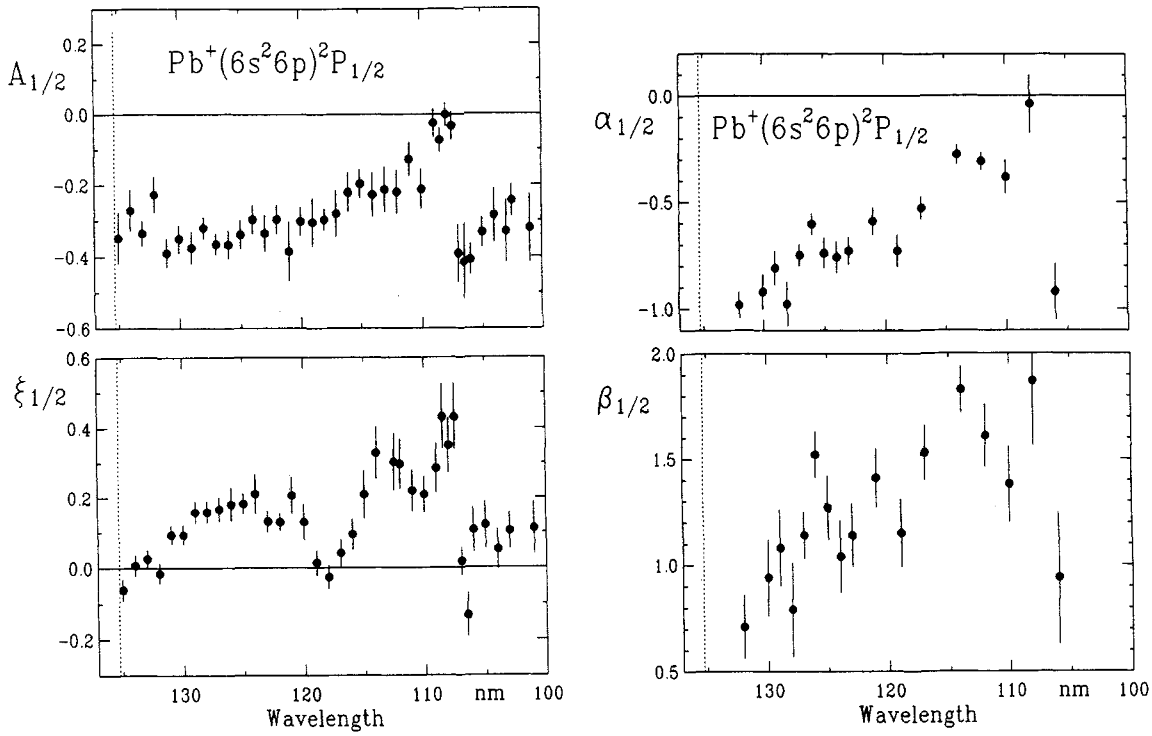

Fig. 2. (a, b) Experimental results (full points with error bars) of the spin-polarisation parameters $A_{1/2}$, $\xi_{1/2}$ and $\alpha_{1/2}$ and the intensity-asymmmetry parameter $\beta_{1/2}$ for photoionisation of $Pb(6s^2 6p^2)_{J=0}$ with final ionic state $Pb^+ (6s^2 6p)\ ^2P_{1/2}$. The vertical dotted line indicates the $^2P_{3/2}$-photoionisation threshold.

ionic channel is observed. Since this resonance is hardly seen in the corresponding photoelectron intensity, which is proportional to the sum of the squares of the dipole-matrix elements $D(\varepsilon s_{1/2})$ and $D(\varepsilon d_{3/2})$ [see equation 3(b)], a strong phase-shift variation [between $D(\varepsilon s_{1/2})$ and $D(\varepsilon d_{3/2})$] is indicated by the "phase-sensitive" $\xi_{1/2}$-parameter [2, 3], possibly as a consequence of an interchannel interaction [22] between the $Pb^+\ ^2P_{1/2}$- and $Pb^+\ ^2P_{3/2}$-continuum states.

The structures of the parameters measured for the $^2P_{3/2}$-ionic channel [see Fig. 3(a, b)] are more pronounced. The values for the spin-polarisation parameter $A_{3/2}$ vary between -0.4 to 0.7. The comparison of the data of the autoioni-

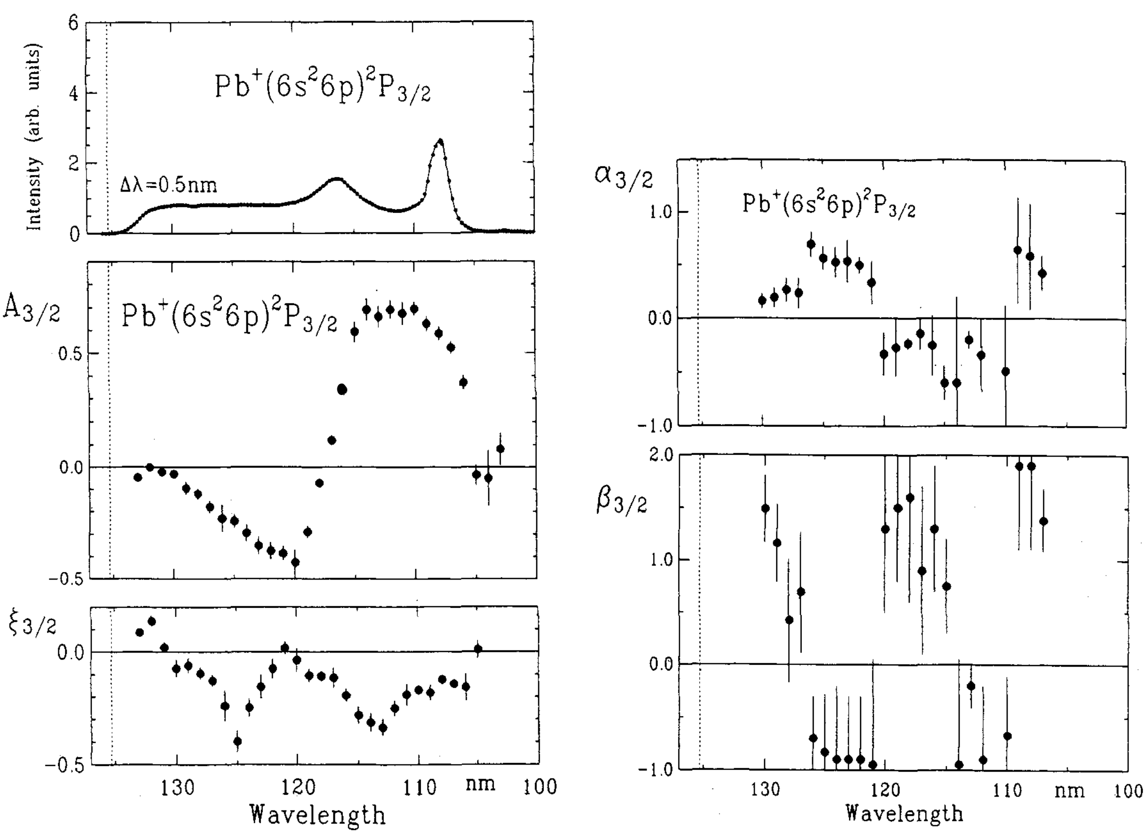

Fig. 3. (a, b) Experimental results (full points with error bars) of the spin-polarisation parameters $A_{3/2}$, $\xi_{3/2}$ and $\alpha_{3/2}$ and the intensity-asymmetry parameter $\beta_{3/2}$ for photoionisation of $Pb(6s^2 6p^2)_{J=0}$ with final ionic state $Pb^+ (6s^2 6p)\ ^2P_{3/2}$. In addition, in (a) the measured photoelectron intensity is shown [see Fig. 1(b)]. The vertical dotted line is the $^2P_{3/2}$-photoionisation threshold.

sation resonances shows that the positions of maxima of the intensity do not correspond to the maxima for the $A_{3/2}$-parameter. The $\xi_{3/2}$-parameters show change in sign in the vicinity of the threshold at $\lambda = 133$ nm as is the case for the $\xi_{1/2}$-parameter. With increasing photon energy the $\xi_{3/2}$-parameter passes through two minima with a variation from -0.4 to 0. A similar structure is observed for the $\alpha_{3/2}$- and $\beta_{3/2}$-parameter. At the extrema for the $\xi_{3/2}$-parameter a strong increase or decrease for these parameters is observed with change of sign for the $\beta_{3/2}$-parameter. The values for the $\beta_{3/2}$-parameter vary between $+1.5$ to -0.95, the asymmetric error bars (also for $\beta_{1/2}$) result from the fact that β is any case limited to values between 2 and -1. We would like to point out that the observed structures of the parameters $A_{3/2}$, $\xi_{3/2}$, $\alpha_{3/2}$ and $\beta_{3/2}$ are much more pronounced than in the measured intensity data.

The high polarisation values measured, up to $A_{3/2} = 0.7$ [see Fig. 3(a)], are not in agreement with the assumption by Radojevic [15] of having collision processes in the target region. If such a scattering mechanism is dominating one would expect a strong decrease of the spin-polarisation of the photoelectrons. Therefore the assignments for the autoionisation resonances given by Radojevic [15] should be modified.

Our further work will concentrate on the evaluation of "experimental" dipole matrix elements and phase-shift differences from the measured data which is expected to clarify these open questions since electron interactions can be seen here more directly [2–6].

Concluding, in the present investigation the three spin-polarisation parameters A, ξ and α were measured for photoelectrons emitted from the Pb($6p^2$) valence orbital in the autoionisation region between the second ionisation threshold Pb$^+$ $^2P_{3/2}$ and $\lambda = 100$ nm. They show pronounced spectral variations for both final ionic states indicating a strong interchannel interaction between channels belonging to different final ionic states.

Acknowledgement

We thank H. W. Klausing and M. Salzmann for technical help and discussions, the staff of BESSY for friendly cooperation, and acknowledge support by the Bundesministerium für Forschung und Technologie (05331 and 431 AX).

References

1. Heinzmann, U., Phys. Scripta **T17**, 77 (1987) (and references therein).
2. Heinzmann, U., J. Phys. B: At. Mol. Phys. **13**, 4353 (1980).
3. Heinzmann, U., J. Phys. B: At. Mol. Phys. **13**, 4367 (1980).
4. Schäfers, F., Schönhense, G. and Heinzmann, U., Z. Phys. **A304**, 41 (1982).
5. Schönhense, G. Schäfers, F., Heckenkamp, Ch. and Heinzmann, U., J. Phys. B: At. Mol. Phys. **17**, L771 (1984).
6. Heckenkamp, Ch., Schäfers, F., Schönhense, G. and Heinzmann, U., Z. Phys. **D2**, 257 (1986).
7. Süzer, S., Banna, M. S. and Shirley, D. A., J. Chem. Phys. **63**, 3473 (1975).
8. Derenbach, H., Kossmann, H., Malutzki, R. and Schmidt, V., J. Phys. **B17**, 2781 (1984).
9. Krause, M. O., Gerard, P., Fahlmann, A., Carlson, T. A. and Svensson, A., Phys. Rev. **A33**, 3146 (1986).
10. Garton, W. R. S. and Wilson, M., Proc. Phys. Soc. **87**, 841 (1966).
11. Krause, M. O., Gerard, P. and Fahlmann, A., Phys. Rev. **A34**, 4511 (1986).
12. Brown, C. M., Tilford, S. G. and Ginter, M. L., J. Opt. Soc. Am. **67**, 1240 (1977).
13. Connerade, J. P., Garton, W. R. S., Mansfield, M. W. D. and Martin, M. A. P., Proc. R. Soc. **A357**, 499 (1977).
14. Heppingstall, R.and Marr, G. V., Proc. R. Soc. **A310**, 35 (1969).
15. Radojevic, V., Phys. Rev. **A36**, 425 (1987).
16. Schäfers, F., Peatman, W., Eyers, A., Heckenkamp, Ch., Schönhense, G. and Heinzmann, U., Rev. Sci. Instrum. **57**, 1032 (1986).
17. Heckenkamp, Ch., Eyers, A., Schäfers, F., Schönhense, G. and Heinzmann, U., Nucl. Instr. Methods **A246**, 500 (1986).
18. Huang, K. N., Phys. Rev. **A22**, 223 (1980).
19. Cherepkov, N. A., Adv. At. Mol. Phys. **19**, 395 (1984).
20. Berkowitz, J., Photoabsorption, Photoionization and Photoelectron Spectroscopy, p. 23 ff, Academic press, New York, San Francisco, London (1979).
21. Fano, U. and Cooper, J. W., Rev. Mod. Phys. **40**, 441 (1968).
22. Starace, A. F., Handbuch der Physik (Edited by W. Mehlhorn), Vol. 31, p. 1, Springer Verlag, Berlin (1982).